J Mater Sci (2007) 42:122–129
DOI 10.1007/s10853-006-1042-3

Spectroscopic analysis of carbonization behavior of wood, cellulose and lignin

Kengo Ishimaru · Toshimitsu Hata · Paul Bronsveld · Dietrich Meier · Yuji Imamura

Received: 2 October 2005 / Accepted: 4 January 2006 / Published online: 9 November 2006

Abstract The surface and bulk chemistry of Japanese cedar (*Cryptomeria Japonica)*, cotton cellulose and lignin samples carbonized at 500–1,000 °C was investigated by elemental analysis, Fourier-transform infrared spectroscopy (FTIR), X-ray photoelectron spectroscopy (XPS) and micro-Raman spectrometry. The objective was to link the original wood components to the final carbonized wood microstructures. The carbonized samples show increasing degrees of order from cellulose to wood to lignin. The cellulose component in the wood strongly affects the ordering of polyaromatic carbons in carbonized wood; this ordering is attributed primarily to the difference in ratio between aromatic and aliphatic carbons and to the amount of cross-linking by ether and carboxylic groups up to 500 °C.

K. Ishimaru (✉)
Central Research Laboratory, Daiwa House Industry Co., Ltd., Nara 6310801, Japan
e-mail: k-ishimaru@daiwahouse.jp

T. Hata · Y. Imamura
Research Institute for Sustainable Humanosphere (RISH), Kyoto University, Uji, Kyoto 6110011, Japan

P. Bronsveld
Department of Applied Physics, Materials Science Center, University of Groningen, Groningen, The Netherlands

D. Meier
Federal Research Centre for Forestry and Forest Products, Institute for Wood Chemistry and Chemical Technology of Wood, Hamburg, Germany

Introduction

Carbonized wood has been used traditionally as an adsorbent to control humidity and purify water. Many papers have discussed the porous structure and adsorption properties of carbonized wood [1–8]. It has been reported that the pore structure and adsorption properties differ depending on the carbonization conditions. Generally, the properties of a carbon material can be linked to its microstructure, consisting of polyaromatic stacks [9]. In addition to estimating the distribution and size of pore structures by gas adsorption experiment, it is important to analyze the microstructure of carbonized wood in order to fully understand the carbonized wood's physical and chemical properties.

The microstructure of a carbon material can be defined as the aggregate form of polyaromatic stacks [10]. The polyaromatic stacks grow in the longitudinal and transverse directions with the decrease of cross-linking between aliphatic carbons and ether groups. In non-graphitizable carbons such as carbonized wood, generally the alignment of polyaromatic stacks is disturbed by the development of cross-linking among them at the early stage of carbonization [11, 12]. Therefore, it is important to study and characterize the microstructures of polyaromatic stacks and functional groups of carbonized wood.

The molecular structure and chemical composition of the precursor in the carbon materials formed under solid-phase carbonization affect the degrees of alignment and growth of polyaromatic stacks [13]. Wood is a natural composite of cellulose, hemi-cellulose, and lignin, which are bonded chemically in a rather complex way [14]. It has been reported that the microstructure of carbonized wood is not the same as the original

microstructures of cellulose and lignin [15, 16]. Therefore, the influence of the original components on the microstructure of carbonized wood is complex.

Spectroscopic and microscopic analysis is a suitable approach for the characterization of carbon materials [9, 11]. A TEM study revealed that wood carbonized at a temperature of 700 °C had a mainly amorphous microstructure with some nano-diamond structures [17, 18]. Raman spectroscopy and X-ray photoelectron spectroscopy (XPS) have frequently been used to characterize the surface chemistry and degree of disorder of the polyaromatic stacks [19–28]. In particular, Fourier transform infrared spectroscopy (FTIR) has been used to detect non-aromatic functional groups as the cause of cross-linking in the early stage of carbonization [11, 12]. Few studies have spectroscopically examined the influence of wood constituent components on the microstructure of carbonized wood, especially at the early stage of carbonization from 500 °C to 1,000 °C. In this study, we investigated the structural changes in polyaromatic structures and non-aromatic functional groups together with the disorder degree of the polyaromatic stacks of carbonized forms of wood, cellulose, and lignin in the temperature range of 500–1,000 °C with elemental analysis, FTIR, XPS, and Raman spectroscopies.

Experimental

Samples and carbonization

The raw materials used in this work were sapwood from a 50-year-old Japanese cedar (*Cryptomeria Japonica*), commercial cotton cellulose fiber (Sanyo Mengyo Co. Ltd.) and organosolve lignin powder (200 mesh pass, Alcell Technologies). These raw materials were dried at 105 C for 24 h in an oven and heated with a heating rate of 4 C/min to 500, 600, 700, 800, 900, and 1,000 °C and kept constant for 1 h in a laboratory-scale electric furnace under a nitrogen atmosphere.

Elemental analysis

Elemental analysis of carbon, hydrogen, and oxygen (by difference) of carbonized samples was carried out in a Perkin-Elmer CHN2400 instrument.

Surface spectroscopic characterization

An FTIR-attenuated total reflection (ATR) technique was used to analyze the functional groups in the samples. Spectra were recorded in the range of 4,000–450 cm^{-1} with a resolution of 4 cm^{-1} by using a Perkin-Elmer Spectrum One spectrometer.

The carbonized samples for XPS and Raman measurements were placed on double-sided adhesive-carbon tape mounted on the sample holder. XPS spectra of carbonized samples were obtained with an AXIS-HS (Shimadzu/Kratos) photoelectron spectrometer using non-monochromatised Mg Kα radiation (1253.6 eV), the source of which was operated at 15 kV and 10 mA. The vacuum pressure during the analysis was always lower than 2.0×10^{-7} Pa. High-resolution scans were performed at 40 eV pass energy for the C_{1s} and O_{1s} spectra. The binding energy scale was corrected by referring to the polyaromatic peak in the C_{1s} spectrum as being 284.4 eV. Shirley and linear backgrounds were subtracted from the C_{1s} and O_{1s} spectra. A mixed Gaussian-Lorentzian product function and a single Gaussian function were used for curve fitting of the C_{1s} and O_{1s} spectra, respectively.

The Raman spectra of the carbonized samples were recorded at room temperature with a Renishaw in Via Raman spectroscope equipped with an air-cooled CCD detector. An argon laser (λ = 514.5 nm) was adopted as an excitation source. The laser was focused to approximately 1 μm in diameter at a power of less than 1 mW at the sample surface in order to prevent irreversible thermal degradation. The Raman spectra were recorded more than three times on the same analysis point in order to check sample damage by laser irradiation and were also measured at three different points on a sample. Backscattered Raman spectra were measured in the 1,000–1,800 cm^{-1} zone. The wave number was calibrated using the 520 cm^{-1} line of a silicon wafer.

Results and discussion

Elemental analysis

The variation of H/C and O/C atomic ratios during carbonization for carbonized forms of wood (CW), cellulose (CC), and lignin (CL) was investigated by elemental analysis. Figure 1 shows a van Krevelen diagram by plotting the H/C versus O/C atomic ratios of all samples, which were measured by elemental analysis.

The carbonization processes of CW, CC, and CL were described in terms of three successive stages in the temperature range of 500–1,000 °C. The atomic H/C and O/C ratios behaved most remarkably. From 500 °C to 600 °C, the upper right hand side of the curves in Fig. 1, the O/C ratio of CW, CC, and CL

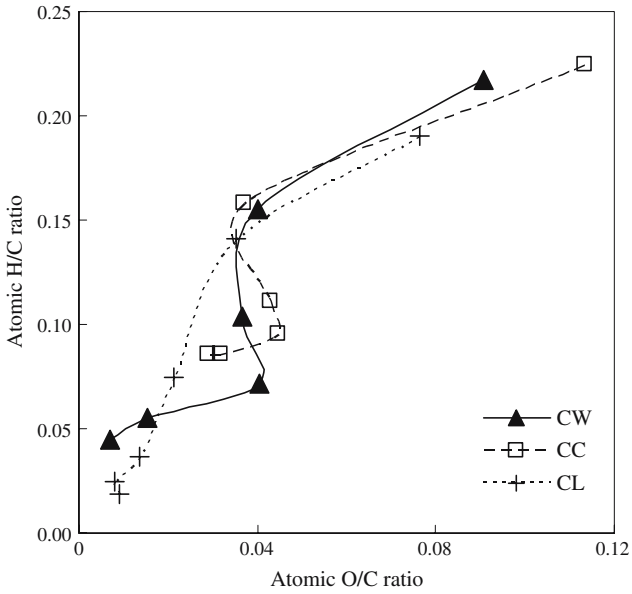

Fig. 1 Van Krevelen diagram. Carbonization paths of the samples: carbonized forms of wood (CW), cellulose (CC), and lignin (CL)

decreased more clearly compared to their atomic H/C ratios. The main reactions in this temperature range were dehydration, decarbonylation, and decarboxylation. In the 600–800 °C range, the more or less vertical middle section in Fig. 1, the atomic H/C ratios decreased more clearly than the atomic O/C ratios. Demethanation and dehydrogenation are the main reactions at this stage. In the range of 800–1,000 °C, the lower left hand side of the curves in Fig. 1, the atomic O/C ratios decreased more significantly than the H/C, indicating that dehydration, decarbonylation, and/or decarboxylation were again the major reactions. Generally, oxygen-containing functional groups at the edge of polyaromatic stacks become volatile when their alignment changes [11, 12]. It is supposed that the polyaromatic stacks were ordered well within the ranges of 500–600 °C and 800–1,000 °C.

At 500 °C, the far right hand points in Fig. 1, the highest values for the atomic H/C and O/C ratios are in the sequence CC, CW, and CL. This is in good agreement with the atomic O/C ratios of 0.90, 0.72, and 0.32 corresponding to cellulose, wood and lignin before carbonization. This agreement is attributable to the fact that in oxygen-rich raw materials, oxygen-containing functional groups develop and polyaromatic stacks become cross-linked [11, 12]. These high atomic O/C ratios for CC, CW and CL before carbonization strongly favored the development of oxygen-containing functional groups, and, for that matter, cross-linking in the carbonized materials.

In the formation of polyaromatic stacks in carbonaceous materials at around 500 °C, it is important to know the chemical structure related to the degree of development of polyaromatic stacks and to the degree of cross-linking during carbonization at that temperature [11, 12]. Therefore, the chemical structures of CW, CC, and CL at 500 and 600 °C were studied in detail by FTIR-ATR.

Fourier transform infrared spectroscopy

Figure 2a shows FTIR-ATR spectra from 600–1,800 cm^{-1} for CW, CC, and CL at 500 °C. The attribution of each band is as follows: 1710 cm^{-1}, C=O stretching vibrations; 1,590 cm^{-1}, aromatic C=C or carbonyl groups conjugated with aromatic structures; 1,440 cm^{-1}, the overlapping peak of C=C and C–H vibrations; 1,350 cm^{-1}, O–H and C=O vibrations; 1,250 cm^{-1}, ether bridges between aromatic rings; 1,150 cm^{-1}, C–O vibrations; 1,050 cm^{-1}, the primary C–OH vibration; and 900–700 cm^{-1}, aromatic C–H vibrations [11, 12, 29, 30]. In the FTIR-ATR spectra at

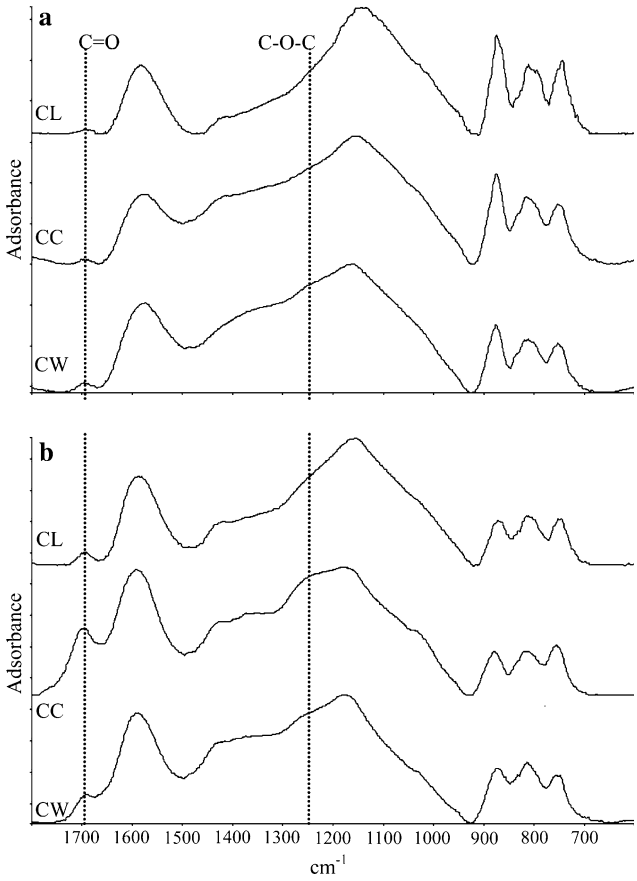

Fig. 2 FTIR-ATR spectra of CW, CC, and CL: (**a**) carbonized at 500 °C, (**b**) carbonized at 600 °C

500 °C, the peaks of oxygen-containing functional groups were observed for CW and CC but less so for CL.

Ether bridges between aromatic rings at the band of 1,250 cm^{-1} and C=O stretching vibrations at 1,710 cm^{-1} were observed clearly in the FTIR-ATR spectra for CW and CC but not so much for CL, as shown in Fig. 2a. The ether bridges between aromatic rings stand for the cross-linking of polyaromatic stacks disturbing the stacks' orientation and development [11, 12]. The C=O structure is also closely related to the cross-linking of polyaromatic stacks in order to lead to an aromatic C–H structure capable of forming cross-linked polyaromatic stacks [11, 12, 31]. The reason why cross-linking of CW and CC developed at 500 °C was that the more disordered the microstructure of a sample was, the more strongly the band for C=O appeared in the FTIR spectra at around 500 °C [11, 12].

The absorption bands of the aromatic C=C at 1,590 cm^{-1}, the overlapping peak of C=C and C–H vibrations at 1,440 cm^{-1}, the C–O vibrations at 1,150 cm^{-1}, and the aromatic C–H vibrations between 900 cm^{-1} and 700 cm^{-1} [11, 12, 29, 30] were obviously observed in FTIR-ATR spectra for CW, CC, and CL at 600 °C, as shown in Fig. 2b. Due to the C=O stretching vibrations at 1,710 cm^{-1}, the O–H and C=O vibrations at 1,350 cm^{-1}, the ether bridges between aromatic rings at 1,250 cm^{-1}, and the primary C–OH vibration at 1,050 cm^{-1}, the peak intensity of the bands decreased significantly according to the FTIR-ATR spectra for CW, CC, and CL at 500–600 °C. This is the logical consequence of the fact that a large number of oxygen-containing functional groups and cross-linking of polyaromatic stacks decompose and volatilize in this temperature range.

The shoulder between 1,300 cm^{-1} and 1,150 cm^{-1} originating from the oxygen functions was clearly observed in the FTIR-ATR spectra for CW and CC but less so for CL. This shows that oxygen-containing functional groups and cross-linking are more developed for CW and CC than for CL at 600 °C; this developmental difference has a strong effect on the degree of disorder of polyaromatic stacks during carbonization.

XPS

The chemical structures of CW, CC, and CL from 500 °C to 1,000 °C were investigated by XPS, which gives accurate information on the surface chemistry of carbonaceous materials up to a depth of 5 nm. The surface O/C atomic ratios of CW, CC, and CL measured by XPS were compared with those of bulk samples measured by elemental analysis, as shown in Fig. 3, in order to determine the potential influence of adsorbed water and/or oxygen in XPS spectra. The surface O/C atomic ratios for CW, CC, and CL tended to be higher than those of the bulk samples. Similar tendencies were reported for coal and wood charcoal [23, 32]. The surface O/C atomic ratios for CW, CC, and CL are higher than the bulk due to the existence of adsorbed water and/or oxygen on the sample surface.

The chemical structure was discussed by curve fitting the O_{1s} peaks for CW, CC, and CL. Figure 4 shows the O_{1s} spectra of CW from 500 °C to 1,000 °C. As there is a more than negligible contribution of adsorbed oxygen and/or water on the sample surface, as shown in Fig. 3, the O_{1s} spectra for CW, CC, and CL were fitted to three peaks as depicted in Fig. 5: a peak for C=O type oxygen (C=O and C<u>O</u>OR; 530.9–531.9 eV), another for C–O type oxygen (C–OH, C–O–C, and CO–<u>O</u>–R; 532.6–533.9 eV) and a third assigned to oxygen atoms in adsorbed oxygen and/or water (535.2–536.4 eV) [21, 23, 33]. Table 1 shows the relative area of C=O, C–O, and adsorbed oxygen and/or water for CW, CC, and CL.

With respect to the chemistry of oxygen-containing functional groups such as C=O and C–O, little change was observed in the relative concentrations between C=O- and C–O- type oxygen of CL at 500–1,000 °C. For CC, the relative area of C–O-type oxygen increased and that of C=O-type oxygen decreased with increasing heat treatment temperature. The relative

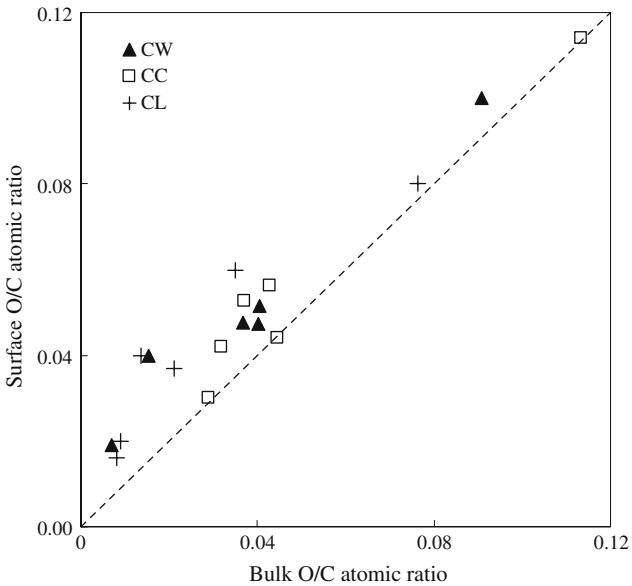

Fig. 3 Comparison of surface O/C atomic ratio by XPS with bulk analysis for CW, CC, and CL

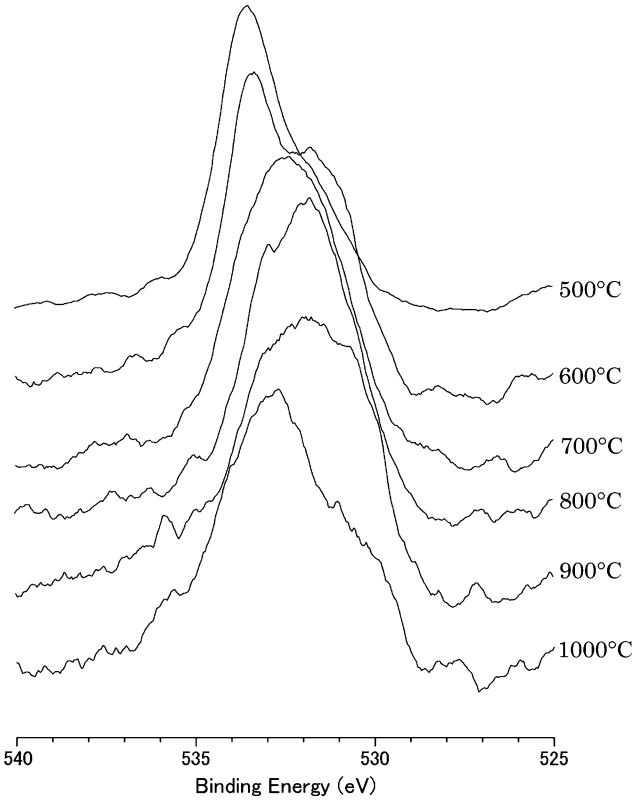

Fig. 4 XPS O_{1s} spectra of CW carbonized from 500 °C to 1,000 °C

concentrations of C=O- and C–O- type oxygen for CW were within the range for CC and CL regardless of temperature. Thus one may conclude that the types of oxygen containing functional groups for CW are similar to those for CC and CL.

From the XPS data in Table 1 as well as from the FTIR-ATR curves in Fig. 2, it is clear that the relative

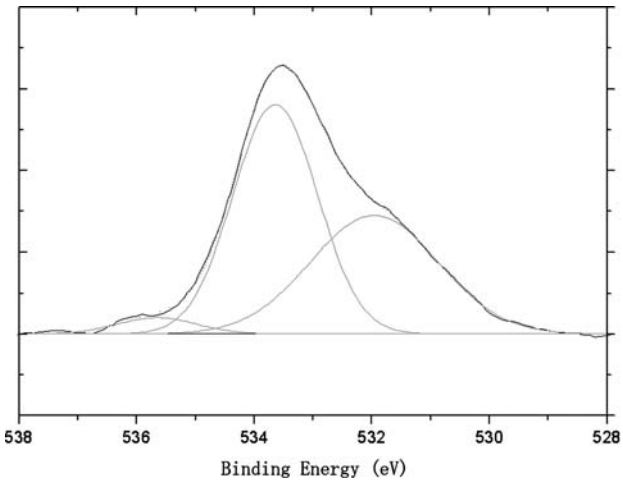

Fig. 5 XPS O_{1s} spectrum observed and calculated by curve fitting of CW carbonized at 500 °C

Table 1 Relative areas of the XPS O_{1s} peaks for CW, CC, and CL by O_{1s} spectra

Sample	HTT(°C)	Components		
		C=O	C–O	CO & H_2O
CW	500	42.4	53.8	3.8
	600	42.5	54.4	3.1
	700	42.5	53.2	4.3
	800	41.2	53.3	5.5
	900	41.9	49.7	8.4
	1,000	35.6	54.5	9.9
CC	500	57	40	3
	600	51.4	47.1	1.6
	700	35.7	57.9	6.4
	800	29.2	61.5	9.3
	900	28.5	63.2	8.3
	1,000	27.1	67.3	5.6
CL	500	41.8	51.8	6.4
	600	41.4	51.6	6.9
	700	45.8	48.8	5.4
	800	42.7	49.8	7.5
	900	48.4	43.8	7.8
	1,000	45.7	51.7	2.6

concentration of C=O- type oxygen for CC was higher than those for CW and CL up to 600 °C. The O_{1s} spectra for carbonized samples showed that cross-linking of polyaromatic stacks for CC develops more than those for CW and CL at 500–600 °C.

The chemical bond of carbon atoms was studied for CW, CC, and CL by curve fitting the C_{1s} spectra. Figure 6 shows the C_{1s} spectra of CW at 500–1,000 °C. Previous authors fitted the C_{1s} spectrum to a polyaromatic peak, symmetric peaks for functional groups, and a plasmon peak [34, 35]. Some papers have added an additional peak around 285.0 eV for carbon in aliphatic and small aromatic structures [21, 22, 36]. This peak was added for the curve fitting because the bands of aliphatic carbon were clearly detected in the FTIR-ATR spectra of CW, CC, and CL at 500 and 600 °C, as shown in Fig. 2. The C_{1s} spectra were fitted to six peaks, as depicted in Fig. 7: a peak for polyaromatic carbons (C–C, 284.4 eV), for aliphatic and small aromatic carbons (C–H, 285.0–285.3 eV), for carbon singly bonded to one oxygen atom (C–O, 286.0–286.4 eV), for carbon doubly bonded to one oxygen or singly bonded to two oxygen atoms (C=O or O–C–O, 287.2–287.9 eV), for carboxylate groups (O–C=O, 288.7–289.2 eV), and a peak for the plasmon (290.7–291.5 eV). Table 2 shows the relative area of each component obtained by curve fitting of the C_{1s} spectra for CW, CC, and CL.

The intensity of the polyaromatic carbon peak is the strongest in the C_{1s} spectra for CW, CC, and CL from 500 °C to 1,000 °C. From 500 °C to 600 °C, the relative concentration of the polyaromatic carbon peak

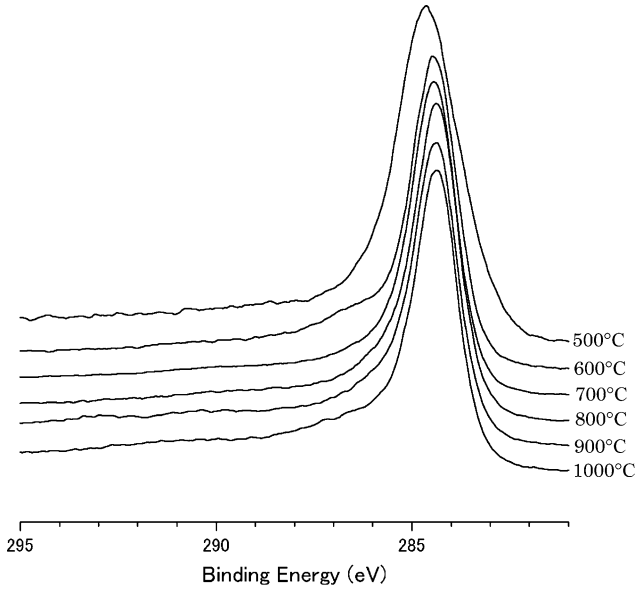

Fig. 6 XPS C_{1s} spectra of CW carbonized from 500 °C to 1,000 °C

increased remarkably for all three samples, indicating that the microstructure is composed mainly of polyaromatic carbons between 500 °C and 600 °C.

On the other hand, especially at 500 °C, a non-negligible contribution of aliphatic and small aromatic carbons was observed in the C_{1s} spectra of CW, CC, and CL as shown in Table 2. The relative areas of aliphatic and small aromatic carbon peaks for CW and CC were higher than that for CL, which means that at 500 °C the cross-linking among polyaromatic carbons is developed more in CW and CC than in CL.

The relative concentration of aliphatic and small aromatic carbons decreased remarkably from 500 °C to 600 °C and was hardly observable above 800 °C, as depicted in Table 2. This is in good agreement with the variation in the atomic H/C ratio from 500 °C to 800 °C. Most of the cross-linking by aliphatic and small aromatic carbons was broken up at 800 °C, reflecting the improvement in the order of polyaromatic stacks above 800 °C.

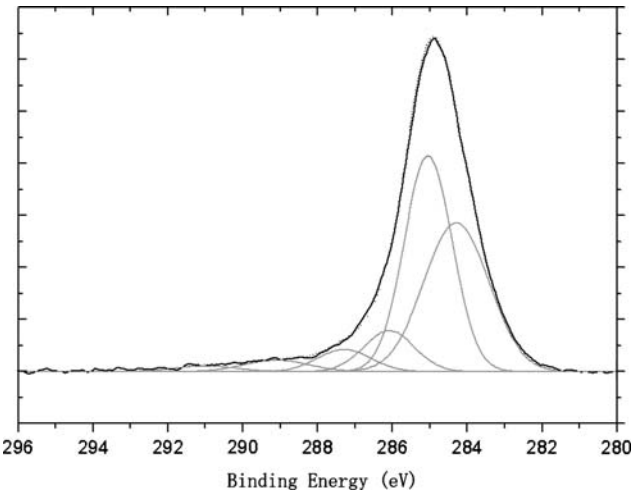

Fig. 7 XPS C_{1s} spectrum observed and calculated by curve fitting of CW carbonized at 500 °C

Raman spectroscopy

Raman spectroscopy was used for a detailed investigation of the degree of ordering of polyaromatic stacks in carbonized samples. Figure 8 shows the Raman spectra of CC from 500 °C to 1,000 °C. Raman bands of carbonized samples appeared at the positions of approximately 1,350 and 1,600 cm^{-1}, corresponding to the in-plane vibrations of sp^2-bonded carbon with structural imperfections (D band) and to the in-plane vibrations of the sp^2-bonded crystalline carbon (G band), respectively [37–40]. Moreover, a ''D'' band at the position of approximately 1,525 cm^{-1} and a shoulder at about 1,190 cm^{-1} were observed. The Raman peaks were extracted using these four peaks, giving a good fit [24, 41]. The full width at half maximum (FWHM) of the D band was used as the major parameter to estimate the disorder degree of polyaromatic stacks [41]. Figure 9 shows the FWHM of the Raman D bands for CW, CC, and CL as a function of heat treatment temperature. The FWHM decreases with temperature and thus decreases as the degree of ordering for polyaromatic stacks increases.

The disorder degrees of the polyaromatic stacks in CW, CC, and CL clearly decreased from 500 °C to 600 °C and from 800 °C to 1,000 °C, as shown in Fig. 9. From 500 °C to 600 °C, the decrease results from the formation of polyaromatic stacks, the breaking of cross-links, and the volatilization of oxygen-containing functional groups, as shown in Figs. 1 and 2 and in Table 2. From 800 °C to 1,000 °C, the decrease is due to the destruction of the cross-linking of the aliphatic and small aromatic carbons that occurs (i.e., the cross-linking occurs) between polyaromatic stacks up to 800 °C, as shown in Table 2.

At each heat treatment temperature, the FWHM of the Raman D band for CL had the lowest value, whereas in all samples the corresponding value for CC was the highest (Fig. 9). The value for CW was intermediate between CC and CL. The degrees of cross-linking development for CW, CC, and CL from 500 °C to 600 °C are described in ascending order as CC, CW, and CL (Figs. 1 and 2). The disorder degree of polyaromatic stacks is lower for CL than for CW and CC, as shown in Fig. 9. On the other hand, the disorder

Table 2 Relative areas of the XPS C_{1s} peaks for CW, CC, and CL

Sample	HTT(°C)	Components					
		Polyaromatic carbon	Aliphatic and small aromatic carbon	C–O	C=O	COOH	Plasmon
CW	500	49.1	30.2	11.1	3.8	4.2	1.6
	600	71.9	6.7	9.8	5.1	4.1	2.4
	700	74.9	4.4	9.8	4.3	3.9	2.7
	800	77.9	0.7	9	5.7	4	2.7
	900	77	1	10	4.7	3.5	3.5
	1,000	73.4	0.7	13.6	4.2	4.2	3.9
CC	500	36.6	30.3	18.7	7.6	4.8	1.7
	600	71.3	7.2	11.1	3.8	4.4	2.3
	700	68.4	3.3	15.2	5.7	4	3.4
	800	66.6	2.8	14.1	9.4	3.8	3.4
	900	75	0.4	12.1	5.6	3	3.7
	1,000	79.2	0.5	9.4	4.8	2.8	3.4
CL	500	53.9	19.9	16.5	4	3.6	1.8
	600	68.7	8.6	11.4	4.7	3.5	3.1
	700	66.8	4.4	12.8	8.5	3.6	3.7
	800	65.1	1.4	13.1	12.6	3.9	3.6
	900	76.5	0	7.4	7.4	4.2	4.1
	1,000	79.4	0	8.1	4.6	4	3.9

degree of the stacks for CW was closer to that of CC than to that of CL. This is attributable to the fact that the development degrees of cross-linking of oxygen-containing functional groups as well as of aliphatic and small aromatic carbons of CW are almost the same as those of CC (Figs. 1 and 2 and Table 2). This implies that the cellulose component in wood strongly affects the formation process for ordering of polyaromatic carbons in CW.

Conclusion

The carbonization behavior of CW, CC, and CL in the range of 500–1,000 °C was studied spectroscopically. A carbonized structure composed mainly of polyaromatic

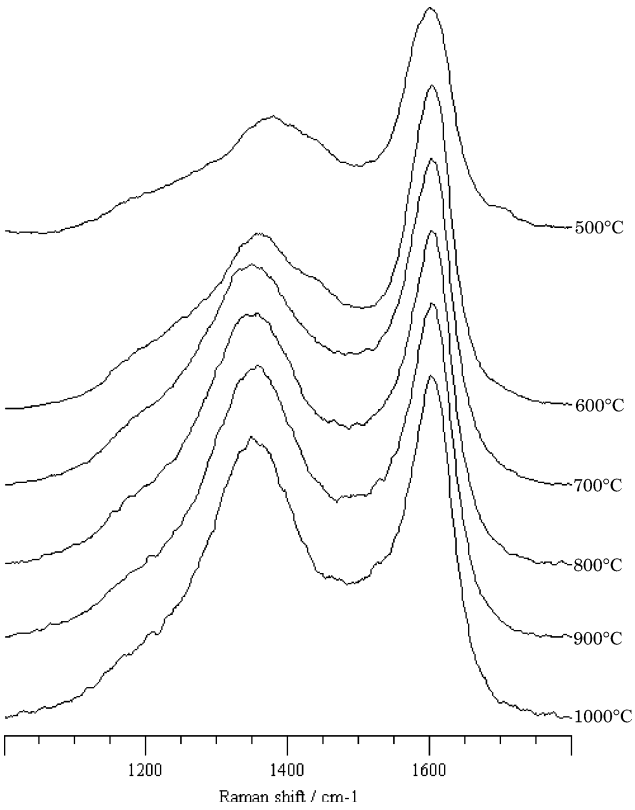

Fig. 8 Raman spectra of CC carbonized from 500 °C to 1,000 °C

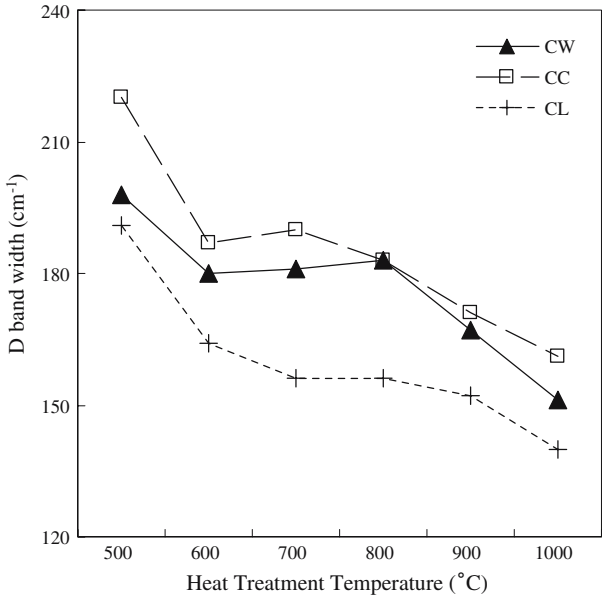

Fig. 9 Effects of heat treatment temperature on the FWHM (Raman D band) for CW, CC, and CL

carbon was formed due to the decomposition and volatilization of non-aromatic functional groups up to 600 °C, after which the Raman D-band width of carbon decreased further up to 1,000 °C. The degree of ordering of polyaromatic stacks at each heat treatment temperature is described in the ascending order of CL, CW, and CC. This may be due to differences among CW, CC, and CL in the degree of cross-linking, such as ether bridges and small aromatic structures, in the range of 500–600 °C. It appears that the degree of development of the polyaromatic structures and the cross-linking for CW, CC, and CL during carbonization are closely related to the O/C atomic ratio before carbonization. Byrne and Nagle have proposed a cellulose microfibril dominance model for the formation mechanism of carbonized wood microstructures [25, 42]. It appears that the CW formation mechanism is closer to that of CC than to that of CL. The microstructure in carbonized wood is strongly affected by the composition ratio of carbon to oxygen atoms in wood.

By using these diverse spectroscopic data, we have been able to pinpoint the initial steps in the carbonization process of wood.

Acknowledgements The authors are grateful to Dr. Junji Sugiyama, RISH, for assistance with the FTIR measurements. This research was supported by a Grant-in-Aid for Scientific Research (14002121) from the Ministry of Education, Science, Sports, and Culture of Japan.

References

1. Ehrburger P, Lahaye J (1982) Carbon 20:433
2. Pulido-Novicio L, Hata T, Imamura Y, Ishihara S (1998) J Wood Sci 44:237
3. Pulido-Novicio L, Kurimoto Y, Aoyama M, Seki K, Doi S, Hata T, Ishihara S, Imamura Y (2001) J Wood Sci 47:159
4. Pulido-Novicio L, Hata T, Kurimoto Y, Doi S, Ishihara S, Imamura Y (2001) J Wood Sci 47:48
5. Mori M, Saito Y, Shida S, Arima T (2000) Mokuzaigakkaishi (in Japanese) 46:355
6. Abe I, Fukuhara T, Maruyama S, Tatsumoto H, Iwasaki S (2001) Carbon 39:1069
7. Maruyama K, Takagi H, Kodama M, Hatori H, Yamada Y, Asakura R, Izumida H, Morita M (2003) Tanso (in Japanese) 208:109
8. Asakura R, Morita M, Maruyama K, Hatori H, Yamada Y (2004) J Mater Sci 39:201
9. Thrower PA (1989) In: Chemistry and physics of carbon. Marcel Dekker Inc., New York and Basel, p 2
10. Oberlin A (1984) Carbon 22:521
11. Villey M, Oberlin A, Combaz A (1979) Carbon 17:77
12. Oberlin A, Villey M, Combaz A (1980) Carbon 18:347
13. Mochida I, Ku C, Korai Y (2001) Carbon 39:399
14. Kollmann FFP, Cote WA Jr (1968) In: Principles of wood science and technology I. Springer-Verlag, New York, p 18
15. Greil P, Lifka T, Kaindl A (1998) J Eur Ceram Soc 18:1961
16. Otani S, Oya A (1971) Tanso (in Japanese) 46:10
17. Hata T, Imamura Y, Kobayashi E, Yamane K, Kikuchi K (2000) J Wood Sci 46:89
18. Ishimaru K, Vystavel T, Bronsveld P, Hata T, Imamura Y, De Hosson J (2001) J Wood Sci 47:414
19. Takahagi T, Ishitani A (1988) Carbon 26:389
20. Desimoni E, Casella G, Morone A, Salvi A (1990) Surf Interface Anal 15:627
21. Darmstadt H, Roy C, Kaliaguine S (1994) Carbon 32:1399
22. Nishimiya K, Hata T, Imamura Y, Ishihara S (1996) J Wood Sci 44:56
23. Darmstadt H, Pantea D, Summchen L, Roland U, Kaliaguine S, Roy C (2000) J Anal Appl Pyrolysis 53:1
24. Yamauchi S, Kurimoto Y (2003) J Wood Sci 49:235
25. Paris O, Zollfrank C, Zickler GA (2005) Carbon 43:53
26. Darmstadt H, Roy C (2003) Carbon 41:2653
27. Kurosaki F, Ishimaru K, Hata T, Bronsveld P, Kobayashi E, Imamura Y (2003) Carbon 41:3057
28. Kawamoto K, Ishimaru K, Imamura Y (2005) J Wood Sci 51:66
29. Pastor-Villegas J, Valenzuela-Calahorro C, Bernalte-Garcia A, Gomez-Serrano V (1993) Carbon 31:1061
30. Gomez-Serrano V, Pastor-Villegas J, Perez-Florindo A, Duran-Valle C, Valenzuela-Calahorro C (1996) J Anal Appl Pyrolysis 36:71
31. Fitzer E, Schafer W (1970) Carbon 8:353
32. Perry D, Grint A (1983) Fuel 62:1024
33. Darmstadt H, Roy C, Kaliaguine S, Choi S, Ryoo R (2002) Carbon 40:2673
34. Proctor A, Sherwood P (1982) Surf Interface Anal 4:212
35. Xie Y, Sherwood P (1990) Chem Mater 2:293
36. Darmstadt H, Roy C, Kaliaguine S, Ting J, Alig R (1998) Carbon 36:1183
37. Nakamizo M, Honda H, Inagaki M (1978) Carbon 16:281
38. Green P, Johnson C, Thomas K (1983) Fuel 62:1013
39. Johnson C, Patrick J, Thomas K (1986) Fuel 65:1284
40. Katagiri G, Ishida H, Ishitani A (1988) Carbon 26:565
41. Cuesta A, Dhamelincourt P, Laureyns J, Martinez-Alonso A, Tascon J (1994) Carbon 32:1523
42. Byrne C, Nagle D (1997) Carbon 35:267